Chellu, Abhiroop; Koivusalo, Eero; Raappana, Marianna; Ranta, Sanna; Polojärvi, Ville; Tukiainen, Antti; Lahtonen, Kimmo; Saari, Jesse; Valden, Mika; Seppänen, Heli; Lipsanen, Harri; Guina, Mircea; Hakkarainen, Teemu

GaAs surface passivation for InAs/GaAs quantum dot based nanophotonic devices

Published in:
Nanotechnology

DOI:
10.1088/1361-6528/abd0b4

Published: 26/03/2021

Document Version
Peer-reviewed accepted author manuscript, also known as Final accepted manuscript or Post-print

Please cite the original version:
Chellu, A., Koivusalo, E., Raappana, M., Ranta, S., Polojärvi, V., Tukiainen, A., Lahtonen, K., Saari, J., Valden, M., Seppänen, H., Lipsanen, H., Guina, M., & Hakkarainen, T. (2021). GaAs surface passivation for InAs/GaAs quantum dot based nanophotonic devices. *Nanotechnology*, *32*(13), Article 130001. https://doi.org/10.1088/1361-6528/abd0b4

GaAs surface passivation for InAs/GaAs quantum dot based nanophotonic devices

GaAs surface passivation for InAs/GaAs quantum dot based nanophotonic devices

Abhiroop Chellu[1, *], Eero Koivusalo[1], Marianna Raappana[1], Sanna Ranta[1], Ville Polojärvi[1], Antti Tukiainen[1], Kimmo Lahtonen[2], Jesse Saari[3], Mika Valden[3], Heli Seppänen[4], Harri Lipsanen[4], Mircea Guina[1] and Teemu Hakkarainen[1]

[1] Optoelectronics Research Centre, Physics Unit, Tampere University, Tampere, 33720, Finland

[2] Faculty of Engineering and Natural Sciences, Tampere University, Tampere, 33720, Finland

[3] Surface Science Group, Physics Unit, Tampere University, Tampere, 33720, Finland

[4] Department of Electronics and Nanoengineering, Aalto University, Espoo, 02150, Finland

Email: abhiroop.chellu@tuni.fi

Received

Accepted for publication

Published

Abstract

Several passivation techniques are developed and compared in terms of their ability to preserve the optical properties of close-to-surface InAs/GaAs quantum dots (QDs). In particular, the influence of N-passivation by hydrazine chemical treatment, N-passivation by hydrazine followed by atomic layer deposition (ALD) of AlO_x and use of AlN_x deposited by plasma-enhanced ALD are reported. The effectiveness of the passivation is benchmarked by measuring the emission linewidths and decay rates of photo-carriers for the near-surface QDs. All three passivation mechanisms resulted in reducing the oxidation of Ga and As atoms at the GaAs surface and consequently in enhancing the room-temperature photoluminescence (PL) intensity. However, long-term stability of the passivation effect is exhibited only by the hydrazine + AlO_x process and more significantly by the AlN_x method. Moreover, in contrast to the results obtained from hydrazine-based methods, the AlN_x passivation strongly reduces the spectral diffusion of the QD exciton lines caused by charge fluctuations at the GaAs surface. The AlN_x passivation is found to reduce the surface recombination velocity by three orders of magnitude (corresponding to an increase of room-temperature PL signal by ~1030 times). The reduction of surface recombination velocity is demonstrated on surface-sensitive GaAs (100) and the passivating effect is stable for more than one year. This effective method of passivation, coupled with its stability in time, is extremely promising for practical device applications such as quantum light sources based on InAs/GaAs QDs positioned in small-volume photonic cavities and hence in the proximity of GaAs-air interface.

Supplementary material for this article is available online

Keywords: quantum dots, surface passivation. GaAs (100), spectral diffusion, photoluminescence, quantum-confined Stark effect, surface states

1. Introduction

Self-assembled InAs/GaAs quantum dots (QD) have been extensively researched owing to their enormous potential for applications in versatile optoelectronic devices including lasers [1], solar cells [2] and photodetectors

[3]. They are also promising solid-state sources of non-classical forms of light, such as single-[4,5] and entangled-[6] photons. An important area of research in quantum technology is concerned with engineering single-photon interactions. To this end, coupled QD-cavity systems demonstrate cavity quantum electrodynamics effects such as vacuum Rabi splitting [7], Purcell enhancement [8] and other single-photon level nonlinearities like photon blockade and photon tunneling [9]. Minimization of the cavity volume results in strong QD-cavity interactions in which single QDs interact preferentially with strongly confined optical modes. Nanofabrication is used to design such low cavity-volume structures, albeit with possible losses in emission efficiency introduced by the inadvertent creation of trap states resulting from crystal defects in the areas surrounding the QDs [10]. However, even if the effect of nanofabrication is minimized by careful optimization of the processing steps, there is a fundamental degradation in the optical properties of QDs caused by the inevitable proximity of surfaces to the QDs in small cavity-volume structures [11], ultimately leading to losses in emission efficiency and in spectral purity.

This study is focused on developing an effective and lasting passivation method for InAs/GaAs QDs that are situated close to a GaAs (100) surface. GaAs is known for its notoriously high density of surface states (usually in the order of 10^{13} cm^{-2}), which in turn contributes to high surface recombination velocities. Typical surface recombination velocities for GaAs are relatively high and they can vary from 10^4 cm s^{-1} to 10^9 cm s^{-1} for low, unintentional doping levels of ~10^{15} cm^{-3} to medium to high doping levels of ~10^{17} cm^{-3}, respectively [12]. Surface states are non-radiative in nature and can form traps in the energy structure of the QDs, leading to a loss in the effective number of charge carriers that can participate in radiative recombination. This results in a reduction in the overall emission efficiency of a single-photon device, for example. The proximity of these states to individual QDs also leads to spectral diffusion, blinking and quantum decoherence or dephasing [10] In general, confinement of excitons within single QDs results in very narrow emission linewidths (typically in the order of a few μeV at cryogenic temperatures) as seen in their characteristic photoluminescence (PL) spectra. However, studies have shown that PL emission from single self-assembled QDs exhibit large shifts (up to ~meV) in emission peak position. The origin of these spectral shifts is attributed to the time-dependent quantum-confined stark effect (QCSE) [13–15]. Fluctuating electric fields in the vicinity of QDs randomly shift and broaden the emission peaks. QCSE is henceforth enhanced when there are abundant surface-induced trap states present in the QDs' surroundings that trap the photo-excited charge carriers. Such a spectral diffusion inevitably affects the degree of indistinguishability of emitted photons from single-photon sources, thus limiting device performance. Another parameter that is critical to device performance is the overall brightness of a single-photon source, such as a QD-cavity system, which is determined by its PL characteristic lifetime. The PL lifetime, which is a combination of the radiative and the non-radiative lifetimes of charge carriers, can be engineered by manipulating the characteristics of the cavity. Unfortunately, the non-radiative lifetime component can be significantly decreased due to a variety of unintentional reasons, including the non-radiative losses caused by defects or surface trap states present near QDs. In some extreme cases, the QDs do not emit any PL at all during random periods with ms timescales [16]. Such a PL intermittency, which is called blinking, is a common phenomenon in solid-state quantum emitters [17–21]. In general, blinking in epitaxial QDs is not very pronounced, largely because such QDs are grown in ultra-pure environments and embedded hundreds of nanometers below exposed surfaces. However, as QDs are frequently being incorporated into photonic nanostructures with critical dimensions of tens or few hundreds of nanometers, surfaces play an important role in determining their optical properties [11]. Studies also show that blinking and spectral diffusion are correlated and occur due to the close proximity of surface trap states [22]. These issues can be generally alleviated by reducing the surface states through a passivation procedure.

Surface passivation processes generally replace the native oxide layer by a thin film of inert material that is chemisorbed on the surface. This process effectively reduces the surface state density of bulk GaAs crystals. To this end, the most common procedures studied so far include chemical passivation by sulfide compounds like ammonium sulfide $(NH_4)_2S$ [23] and sodium sulfide Na_2S [24,25] solutions, surface treatment by phosphor-based compounds [26], and chemical nitridation by hydrazine [27,28]. Furthermore, the passivation of the GaAs surface can be achieved also by growing thin layers of AlN_x, AlO_x, TiN_x, HfO_2 or SiN_x by atomic layer deposition (ALD) [29–33]. These passivation techniques have shown improvement of the optical properties of GaAs bulk, InGaAs/GaAs quantum wells and GaAs nanowires, but there is very little research on the effect of surface passivation on the emission properties, such as exciton linewidths and decay rates, of close-to-surface QDs.

In this work, we investigate the impact of different surface passivation techniques on the optical properties of self-assembled InAs QDs close to GaAs (100) surface, aiming at preserving their intrinsic optical properties but also at long-term stability of the passivation process. Namely, we study chemical N-passivation, chemical N-passivation followed by immediate ALD of an AlO_x thin film and ALD-based AlN_x passivation without the

chemical treatment. The passivation effect is assessed by measuring the room-temperature PL of GaAs (100) epilayers and the luminescence features of near-surface InAs QDs, including QD emission linewidths and QD PL decay times.

2. Experimental details

2.1 MBE growth of InAs/GaAs quantum dots

The investigated samples were grown by solid-source molecular beam epitaxy (MBE) on (100) oriented semi-insulating GaAs substrates. The QDs formed through self-assembly in the Stranski-Krastanov growth regime. The nucleation of InAs into 3D islands started after depositing a critical thickness of 1.7 monolayers (ML) of InAs wetting layer (WL) on the GaAs matrix at 530°C. After an overall deposition of 2.1 ML of InAs, the QDs were capped with a thin GaAs layer. Since the thickness of the GaAs cap layer determines the distance between the QDs and the surface, it was varied in order to study the influence of surface proximity on the optical properties of the QDs. For this purpose, we used cap layer thicknesses of 20 nm, 30 nm, 40 nm and 60 nm. An additional sample with uncapped surface QDs was grown under identical conditions for studying the QD density. During QD growth, a gradient of temperature maintained the center of the wafer relatively cooler than the edges. This resulted in a lower QD density by approximately three orders of magnitude when moving radially from the center towards the edge of the sample. The density gradient is useful since it helps in studying micro-photoluminescence (μPL) of individual QDs from low-density areas and PL decay rates of ensemble QDs from high density areas on the same sample. The QD densities in the high-density and low-density areas were assessed using atomic force microscopy (AFM) and μPL imaging, respectively, with exemplary pictures shown in figure 1. Furthermore, a surface-sensitive GaAs epilayer was grown for the room-temperature investigation of PL properties. This sample consisted of a 500 nm GaAs layer, which was separated from the semi-insulating GaAs substrate by a 100 nm GaInP barrier. The purpose of the GaInP barrier is to prevent diffusion of the photo-excited charge carriers from the GaAs epilayer to the substrate during the PL experiments.

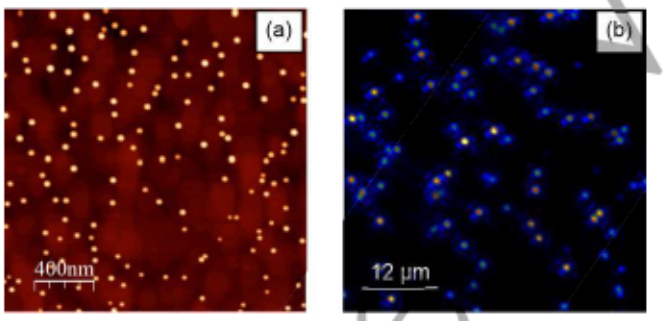

Figure 1. (a) AFM image of InAs QDs from a high-density portion of the sample. QD-ensembles from such high-density regions were studied to estimate carrier decay rates. (b) Photoluminescence image of InAs QDs from a low-density portion of the sample. The PL emission from GaAs bulk and InAs WL have been filtered out to isolate individual QDs to study their excitonic emission linewidths.

2.2 Surface passivation

Three different surface passivation approaches were investigated for near-surface QDs and surface-sensitive GaAs bulk samples. The first passivation approach was hydrazine (N_2H_4) based chemical nitridation of the GaAs surface at room temperature. SH^- anions originating from NaS remove surface As atoms, while N_2H_4 reacts with surface Ga atoms to form a passivating monolayer of GaN. Solution preparation and the subsequent passivation steps were followed according to the procedure presented in [34].

In the second approach, the procedure included the steps carried out in the N_2H_4 passivation followed by a subsequent ALD growth of a 2 nm thick AlO_x overlayer. The ALD process was carried out in a Picosun Sunale ALD R200 Advanced reactor at a substrate temperature of 200°C. Electronic-grade trimethylaluminium (TMA) ($Al(CH_3)_3$; ≥99.9%, CAS 75-24-1, Volatec Oy, Finland), ultrapure Milli-Q® water and N_2 (99.9999%) were used as the Al precursor, O precursor and carrier/purge gas, respectively. The growth rate of ~0.1 nm/cycle was determined on a n-Si (100) (P) reference sample using an ellipsometer. The deposition resulted in an oxygen-poor $AlO_{x\sim1}$ thin film as analyzed from X-ray photoelectron spectroscopy (XPS) Al 2p:O 1s ratio. The samples were cooled in a nitrogen atmosphere after the depositions and before being exposed to ambient air.

The third passivation approach is based on nitridation and included ALD of a 2 nm thick AlN_x layer directly on the GaAs surface. The ALD of AlN_x was carried out through plasma-enhanced atomic layer deposition (PEALD) using a Beneq TFS-500 tool. A process with TMA and ammonia (NH_3) as precursors and N_2 as both the plasma and the carrier gas was used as previously demonstrated in [29] and [30] The surface was pretreated with TMA and N_2 plasma, where TMA reacts with the possible native oxides of the sample and N_2 plasma cleans and nitridizes the surface. The temperature was 200°C and the power of the capacitively coupled remote plasma was 50 W in the pretreatment as well as during the deposition. After the deposition, the samples were cooled down in a nitrogen atmosphere before being exposed to ambient air.

2.3 Photoluminescence experiments

PL experiments performed on surface-sensitive GaAs (100) epilayer before and after passivation were carried out at room temperature. The measurements were made using a PL-mapper equipped with a continuous wave (CW) laser operating at 532 nm. The emitted PL was collected by a spectrometer in which the light is dispersed by a 300 lines/mm grating and detected with a charge-coupled device (CCD) array detector. Low-temperature PL experiments were carried out on QDs situated at varying distances from the GaAs (100) surface. The samples were placed in a closed-cycle helium cryostat and cooled down to 6 K in all low-temperature experiments. µPL was carried out to investigate the effectiveness of different passivation techniques based on the PL linewidths of individual QDs. The QDs were excited using a CW semiconductor diode laser operating at 640 nm. The excitation beam was focused down to a spot size of around 1 µm on the sample using a 50x high N.A. objective lens. This allowed the possibility to study the excitonic emission behavior of spatially isolated QDs. The emitted PL was collected by the same objective and directed to a 750 mm spectrometer. The PL was then dispersed by a 1200 lines/mm grating and detected using a cooled Si CCD camera. The spectral resolution of this setup is ~ 60 µeV. Time-resolved photoluminescence (TRPL) experiments were carried out at 6K on QD ensembles to study the effect of passivation on carrier decay rates. An area of approximately 1 µm in diameter on the sample was excited by a train of 60 ps pulses with a repetition rate of 80 MHz generated by a diode laser operating at 850 nm (resonantly exciting the InAs WL). The temporal resolution of the system is 200 ps as determined from the full width at half maximum (FWHM) of the instrument response function (IRF) (figure S1). The emitted PL was spectrally filtered by the monochromator at 950 nm and collected using a single photon avalanche diode (SPAD). The PL time responses were recorded by time-correlated single photon counting (TCSPC). The decay rates were extracted from the PL time traces by single-exponential fits with iterative convolution in order to deconvolute the contribution of the system response from the measured data.

2.4 X-ray photoelectron spectroscopy

XPS was carried out to investigate the chemical composition of surfaces and interfaces before and after surface passivation. Additionally, passivated samples were studied after certain periods of air exposure to estimate the effective stability of each passivation technique in resisting oxidation. The lens-defined selected-area XPS (SAXPS) was performed by employing a wide-area, non-monochromatized illuminating DAR400 X-ray source (Al Kα, 300 W) and an Argus hemispherical electron spectrometer (Omicron nanotechnology GmbH) that is equipped with micro-channel plate electron multipliers and a 128-channel striped anode detector. The core-level spectra were collected with a pass energy of 20 eV, in a high-magnification lens mode and with an in-lens aperture yielding a circular analysis area of Ø1.93 mm.

3. Experimental Results

3.1 Surface characteristics of passivated samples

The oxidation states of Ga and As were determined from the XPS Ga $2p_{3/2}$ and As $2p_{3/2}$ signals on the native oxide surface, the N_2H_4-passivated surface, the ALD-AlO_x/GaAs interface and the ALD-AlN_x/GaAs interface. The 1117 eV and 1118 eV photoelectron peaks in Ga $2p_{3/2}$ can be attributed to Ga–As and Ga^{3+} oxide, respectively, while the 1323 eV and 1326 eV photoelectron peaks in As $2p_{3/2}$ can be attributed to Ga–As and As^{3+} oxide, respectively. As seen from the data presented in figure 2 and in Table 1, the GaAs native oxide surface contained roughly 50% relative concentration of Ga and As oxides. The N_2H_4 passivation removed all Ga oxides but As was either not fully reduced or it started to oxidize within the 10-minute air exposure during sample transfer from the N_2H_4 passivation setup to the XPS system.

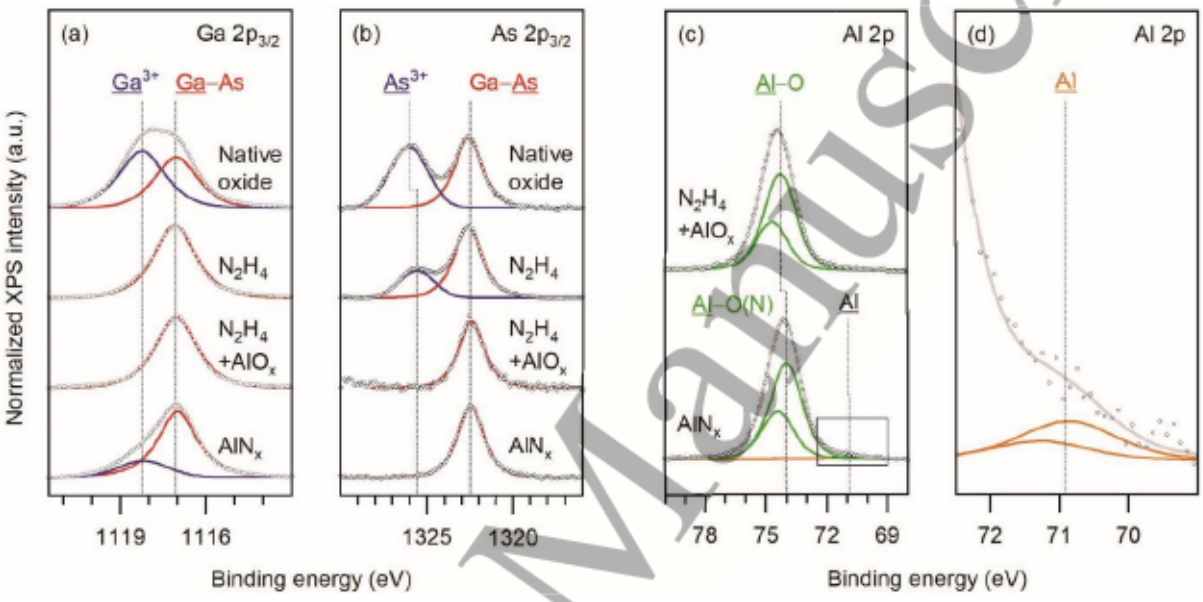

Figure 2. XPS spectra of GaAs (100) surfaces after different passivation treatments. The spectrum of the native oxide on an untreated GaAs surface is presented as a reference. The Ga $2p_{3/2}$, As $2p_{3/2}$, Al $2p_{3/2}$ core-level spectra are shown in (a)-(c), respectively. (d) shows a magnification of the small shoulder of metallic Al indicated by the rectangle in (c). The XPS signals are normalized and the solid line with a peak at 1118 eV in (a) represents Ga^{3+} oxide while the peak at 1326 eV in (b) represents As^{3+} oxide. The N_2H_4 and N_2H_4 + AlO_x passivated surfaces were measured immediately after passivation, while the AlN_x- passivated surface was exposed to air for 152 days before the XPS measurement.

The N_2H_4 passivation combined with ALD-AlO_x passivation layer yielded a fully unoxidized GaAs in the AlO_x/GaAs interface. The N_2H_4 pretreatment removed all Ga oxide and some As oxide, after which the ALD-AlO_x process removed the rest of the As oxide. The passivation resisted oxidation in air for at least 1 week, but after 110 days of exposure to air, both Ga and As were slightly oxidized at the interface. The TMA exposure during ALD is known to reduce As oxides more effectively than the Ga oxides [35]. The AlN_x/GaAs interface resulting from ALD-AlN_x passivation was measured after 152 days of air exposure. Ga was found to be partially oxidized while As remained unoxidized.

To note, the ALD-AlN_x passivation layer combined with TMA and N_2 plasma pretreatment prevents the formation of As oxide longer than the N_2H_4 + ALD-AlO_x passivation does. The ALD-AlO_x layer was oxygen-poor AlO_{x-1} and contained Al only in one chemical state (Al $2p_{3/2}$ oxide at 74.5±0.1 eV). According to the low N/O ratio of around 0.06 and the low N/Al ratio of around 0.09, the ALD-AlN_x layer was also mainly Al oxide (after deposition and long air exposure). It contained Al in two chemical states (Al $2p_{3/2}$ oxide/nitride at 74.0 eV and Al $2p_{3/2}$ metallic at 70.9 eV).

The Al 2p components of Al-O and Al-N cannot be distinguished from each other. The N/O ratio, the chemical shift of -0.5 eV in the main Al 2p peak on ALD-AlN_x compared to ALD-AlO_x and the rather narrow/symmetric peak shape suggest that the film was homogenous 6% N-alloyed Al oxide.

Regarding the small shoulder at 70.9 eV, DuMont et al. have observed a similar small, low binding energy Al 2p component with a more metallic character on a SiO_2 film after TMA exposure. They speculate that the peak may be the result of some TMA decomposition [36]. Therefore, in our case, it most likely originates from the TMA pretreatment. Angle-resolved XPS measurement on ALD-AlN_x showed that the relative amount of metallic Al in Al 2p was 2.3% at 0° and 0.4% at 60° emission. This leads us to conclude that the metallic Al could be confined to the interface.

Overall, compared to the plain AlO_x film, the combination of the N-alloyed AlO_x film with a small amount of metallic Al in the interface acts as a better diffusion barrier which prevents the oxidation of As, especially, for a longer time. This is a considerable difference in the interface chemistry between the ALD-AlN_x and ALD-AlO_x passivated samples considering the important role of As atoms in formation of the detrimental states on GaAs surfaces and in GaAs-Al_2O_3 interfaces [37–42].

Table 1. The relative amounts of unoxidized (Ga^0, As^0) and oxidized (Ga^{3+}, As^{3+}) Ga and As surface atoms estimated from the core level XPS spectra measured after different periods of exposure to air.

Passivation	Storage time in air	Ga^{3+}/Ga_{TOTAL} (Ga $2p_{3/2}$)	As^{3+}/As_{TOTAL} (As $2p_{3/2}$)
Native oxide	–	0.55	0.52
N_2H_4	10 minutes	0	0.30
N_2H_4 + AlO_x	10 minutes	0	0
N_2H_4 + AlO_x	7 days	0	0
N_2H_4 + AlO_x	110 days	0.08	0.17
AlN_x	152 days	0.22	0

3.2 Room-temperature photoluminescence of GaAs epilayer

Bare GaAs surfaces have an abundance of surface states that act as favorable pathways for non-radiative decay of carriers. Thus, comparing the PL intensity before and after surface passivation provides a good indication on the effectiveness of a certain surface passivation mechanism in suppressing the detrimental effects of surface states. Figures 3(a)-(c) shows room-temperature PL spectra of passivated surface-sensitive GaAs epilayers compared with the spectra of the corresponding as-grown GaAs samples taken before each passivation process. Considering the PL intensity from the as-grown sample to be I_0, the improvement in PL emission intensity after N_2H_4 treatment is 634×I_0. The improvement provided by the N_2H_4 + AlO_x passivation turns out to be around 115×I_0, while the AlN_x passivation process provides approximately 1030×I_0. Even though all three passivation mechanisms provide PL enhancement, the most important criterion from a practical viewpoint is the stability of any process, which is presented in figure 3(d) and figure S2 in the supplementary information. To elaborate, the PL measurements were made immediately after carrying out the N_2H_4 and N_2H_4 + AlO_x passivation procedures, while the first spectrum from the AlN_x-passivated sample was measured four days after passivation because of wafer transport. While there was no significant reduction in PL intensity from the AlN_x-passivated samples even after one year, the sample passivated with N_2H_4 is found to degrade rapidly in air exposure. The N_2H_4 + AlO_x passivated sample shows some degradation in one week of air exposure but is still significantly more stable than the sample passivated just by the chemical N_2H_4 process. It is also worth noting that no nitrogen was detected by XPS on the N_2H_4-passivated surface after 10 minutes of exposure to air and 30 minutes in UHV storage. Therefore, it is safe to state that ALD-based passivation methods are more suitable for practical device applications than the chemical N_2H_4 passivation alone since they maintain their positive effects on the GaAs surface for a relatively long period while also providing considerable enhancements in PL intensity.

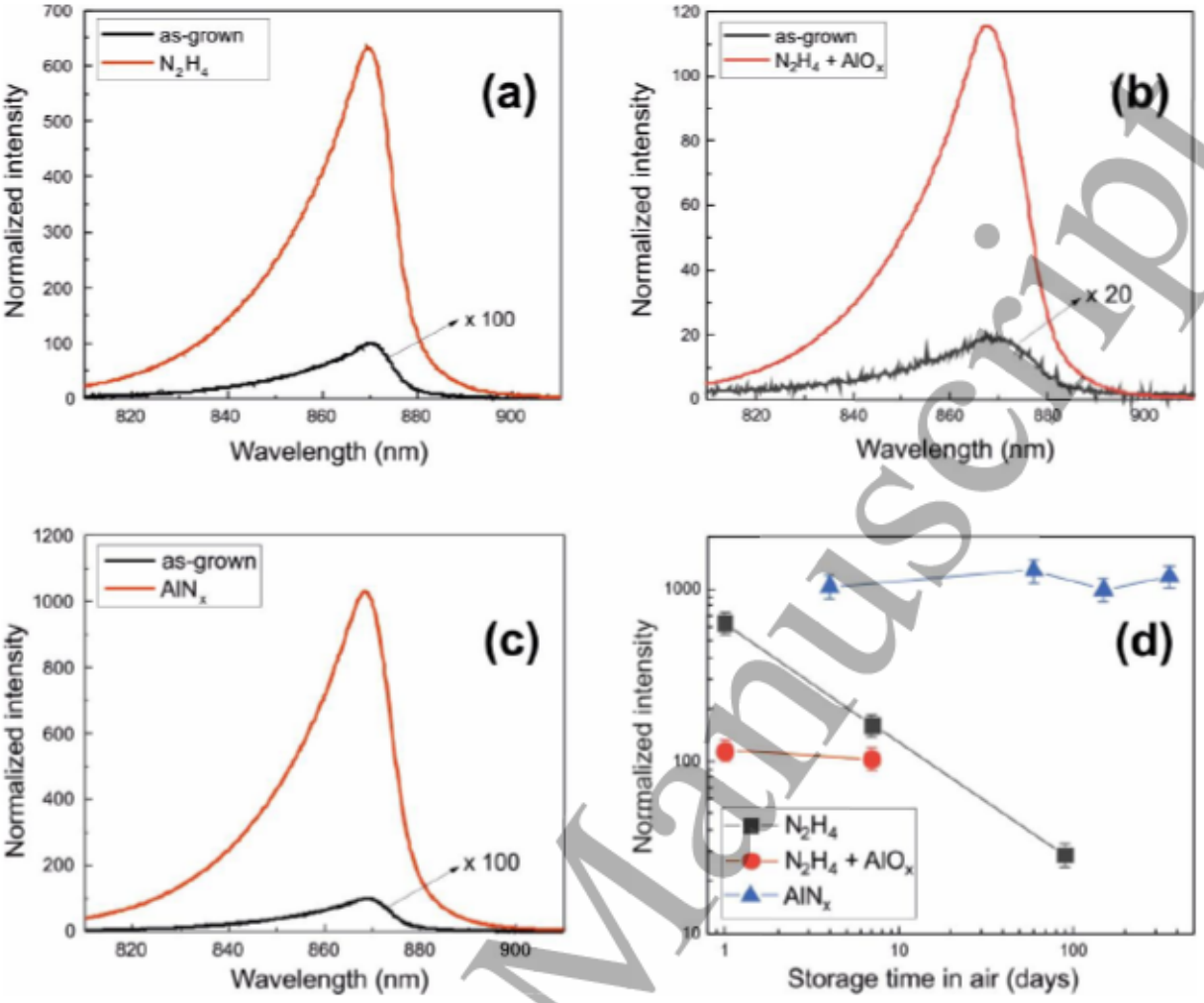

Figure 3. Room temperature PL spectra of surface-sensitive GaAs epilayers measured before and after (a) N_2H_4 passivation, (b) N_2H_4 + AlO_x passivation, and (c) AlN_x passivation. (a) and (b) were measured right after passivation and (c) after a 4-day air exposure. The PL intensity of the passivated GaAs samples are normalized with respect to the as-grown spectra measured from the same samples before passivation. After normalization, the as-grown spectra were multiplied by suitable scaling factors for illustration purposes. (d) shows the stability of the surface passivation as the change in PL peak intensities during air exposure. The storage time of 1 day on the logarithmic scale corresponds to the intensity values recorded right after passivation. The +/- 15% error margins represent the estimated variation in the sensitivity of the PL setup over time.

3.3 Surface recombination velocity

An improvement of more than three orders of magnitude in PL intensity provided by the AlN_x passivation is expected to result from a significant reduction in surface recombination velocity. The dependence of PL intensity I on surface recombination velocity S and on surface depletion layer width W can be expressed as,

$$I = C \exp(-\alpha_e W)\left(\frac{1}{\alpha_e L_p} + \frac{L_p}{S\tau}\right) \quad (1)$$

where, $1/\alpha_e$ is the absorption length (125 nm for a 532 nm excitation in GaAs), L_p is the minority carrier diffusion length and τ is the minority carrier lifetime [43]. Based on the measurement of the surface electric field using a photoreflectance-based method [27,44–46], we infer that the AlN_x passivation has no influence on the surface electric field caused by Fermi-level pinning at the surface states (see figure S3 in Supplementary information). Therefore, assuming that the bulk properties L_p, τ and the level of unintentional doping are unaffected by the

passivation, it is safe to state that the improvement in PL intensity is not due to a change in W, but stems solely from a reduction of surface recombination processes. The improvement in PL intensity provided by AlN_x passivation can thus be expressed as,

$$I/I_0 = \left(\frac{1}{\alpha_e L_p} + \frac{L_p}{S\tau}\right) \Big/ \left(\frac{1}{\alpha_e L_p} + \frac{L_p}{S_0\tau}\right) = 1030 \quad (2)$$

where, S_0 and S are the surface recombination velocities for the as-grown and the AlN_x-passivated surfaces, respectively. The GaAs samples have an n-type background doping level $N_d = 1.3\times10^{15}$ cm^{-3}, as determined from the Hall measurement of a 5 µm undoped GaAs layer grown just before the surface-sensitive GaAs epilayer was grown in the same MBE system. This allows us to use a value of $S_0 = 1\times10^4$ cm s^{-1} [47]. Assuming typical values of n-GaAs with $N_d \sim 1\times10^{15}$ cm^{-3} for minority carrier diffusion length $L_p = 11$ µm and lifetime $\tau = 1.1$ µs, from Equation (2) we get $S = 9$ cm s^{-1}. Thus, we can conclude that AlN_x passivation reduces surface recombination velocity of the GaAs (100) surface by more than three orders of magnitude; S is thus just an order of magnitude larger than the typical interface recombination rate of high-quality GaAs/GaInP interfaces. These values are consistent with our experimental results since we get 20-times higher room-temperature PL intensity from a 500 nm GaAs layer placed between two 100 nm GaInP barriers than from the AlN_x-passivated GaAs surface that has a GaInP barrier just below it. Nevertheless, to our knowledge, these results for AlN_x passivation show the largest reduction of surface recombination in GaAs (100) and the highest improvement of PL intensity reported so far for any post-growth passivation method.

3.4 Photoluminescence linewidth

Low-temperature µPL spectra obtained from individual QDs before and after carrying out different surface passivation treatments are presented in figure 4. Considering the spectra from the as-grown samples in figure 4(a), for a GaAs cap thickness of 60 nm, we observe narrow exciton lines associated with typical PL emission from a QD. The emission lines become broader as the cap thickness is reduced, and at 20 nm we observe very pronounced spectral diffusion. The spectral diffusion is so significant that individual exciton lines are no longer discernible. This inhomogeneous linewidth broadening is attributed to QCSE, where the photo-excited charge carriers (trapped by nearby surface states) induce a local electric field around the QDs that consequently leads to local fluctuations in emission energies. The N_2H_4-passivated QD situated at 60 nm from the GaAs surface exhibits slightly broadened exciton lines, as shown in figure 4(b). From the same figure, it is also easy to note that the QDs situated closer to the surface show a similar, if not a more pronounced spectral diffusion, than as seen in the as-grown QDs. Figure 4(c) shows the excitonic spectra of individual QDs passivated by $N_2H_4 + AlO_x$. The spectral diffusion is quite significant even for the QD situated at 60 nm from the surface. The notable resemblance between the spectra of the $N_2H_4 + AlO_x$ -passivated QD situated at 60 nm (from the surface) in figure 4(c) and the as-grown QD at 20 nm in figure 4(a) suggests a bigger influence of the surface on QDs that are passivated with $N_2H_4 + AlO_x$. On the other hand, AlN_x passivation reduces the exciton linewidths of individual QDs situated 30 nm or more from the GaAs surface. As seen in figure 4(d), the AlN_x-passivated QD situated at 20 nm from the surface exhibits noticeable spectral diffusion but the QDs situated further away depict spectra that are narrow enough to be at (or possibly, even below) the spectral resolution of the measurement system. By comparing the multiplication factors used for the spectra in figures 4(a)-(d), it is clear that while the N_2H_4 and $N_2H_4 + AlO_x$ passivation methods do not have a positive influence on the single QD PL intensity, the AlN_x passivation provides a significant improvement.

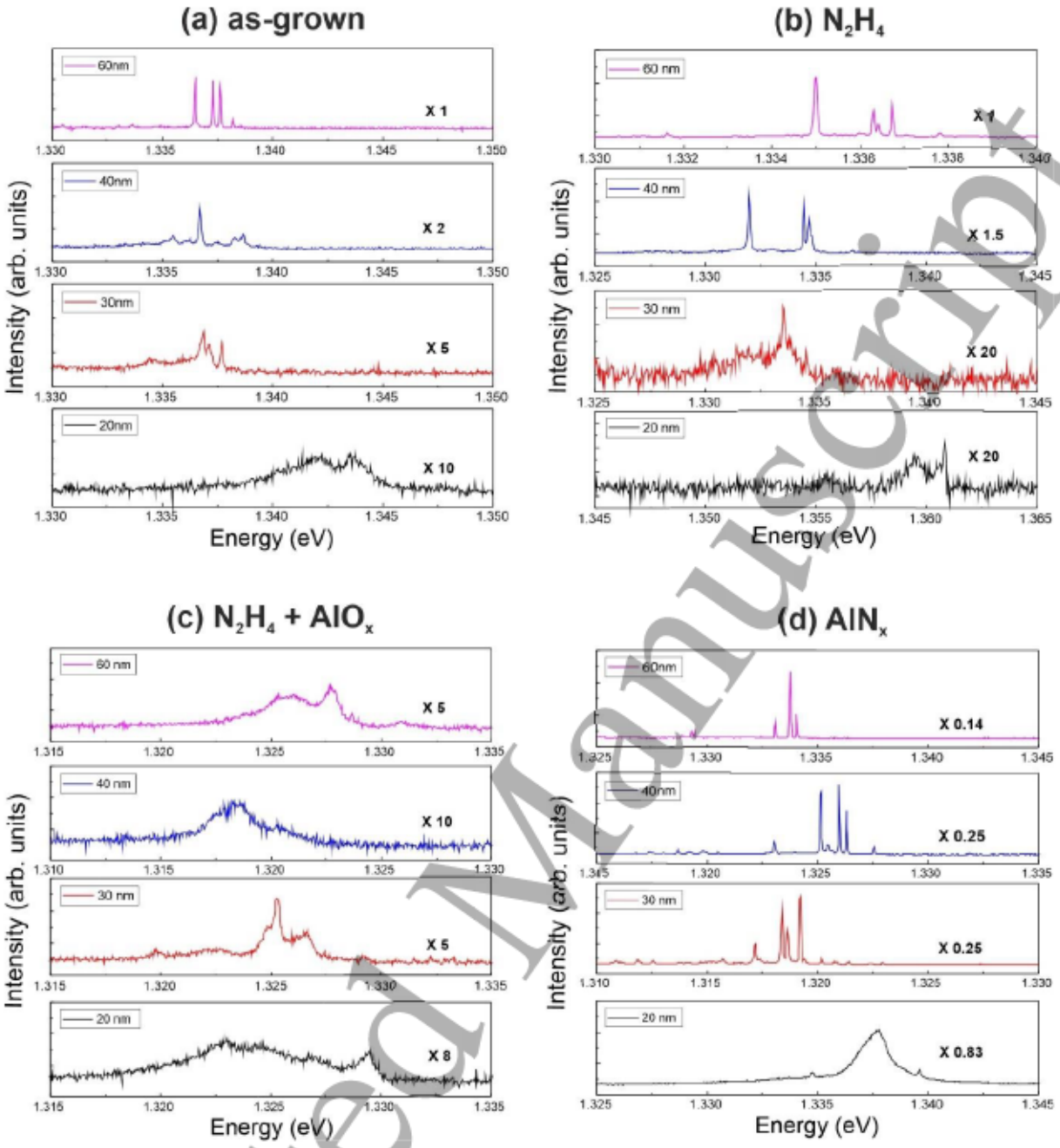

Figure 4. Excitonic spectra of individual QDs capped with 20 nm, 30 nm, 40 nm and 60 nm thick GaAs layers. (a) before surface passivation, (b) after N_2H_4 passivation, (c) after N_2H_4 + AlO_x passivation and (d) after AlN_x passivation. The intensities have been scaled with multiplication factors, which are shown in each individual plot, in order to make qualitative comparison of their linewidths easier. The multiplication factors are inversely proportional to the PL intensity of each QD in comparison with the as-grown QD with 60 nm cap thickness.

A more quantitative representation of the improvement in exciton linewidths and intensities of the AlN_x-passivated QDs over the as-grown QDs is shown in figure 5. It is evident that the differences between the as-grown and AlN_x-passivated samples are considerably larger than the QD-to-QD variation. The exciton peak intensities are at least an order of magnitude higher for the AlN_x-passivated QDs and the peak widths are consistently lower compared to the as-grown QDs. The only exception to this trend is seen in the linewidths of the QDs capped with 20 nm of GaAs, which show very large variations due to the proximity of the surface. Nevertheless, the data presented in figure 5 is a clear indication of (i) successful suppression of the surface-induced spectral diffusion and (ii) reduction of the non-radiative loss of photo-excited electron-hole pairs caused by surface recombination (before they are eventually captured by the QDs) for cap thicknesses of 30 nm or more.

Remarkably, except for the 20 nm cap sample, the exciton linewidth and the emission intensity of AlN_x-passivated QDs have a very weak dependence on the distance.

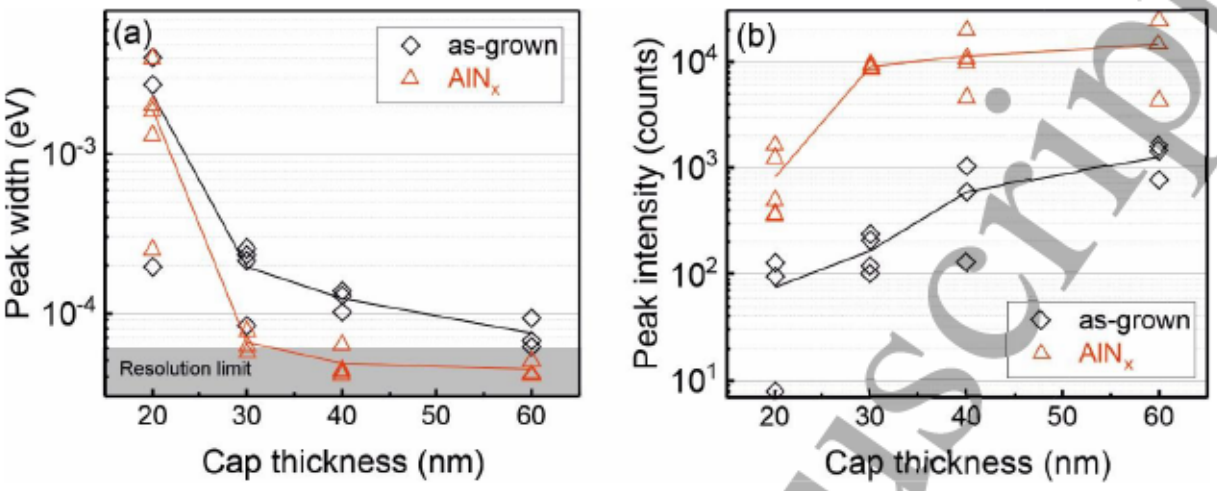

Figure 5. Linewidths (a) and integrated intensities (b) of the dominant exciton peaks extracted from single QD spectra of 3 - 5 QDs per sample for as-grown and AlN_x-passivated QD samples. The solid lines represent the mean values.

3.5 Photoluminescence decay rate

The PL intensity from bulk GaAs and the exciton peak intensities measured from individual QDs that are presented in the previous sections are strongly dependent on the non-radiative processes at the GaAs surface. In order to investigate radiative and non-radiative processes in the QDs themselves, we employ TRPL to probe the decay of the photo-excited electron-hole pairs in the QDs. It should be noted that the measured PL decay rates include both the radiative and the non-radiative components. The radiative component is due to the spontaneous emission of photons, which occurs through exitonic decay and the decay rate is governed by the intrinsic properties of radiative transition and by the local density of optical states (LDOS) of the dielectric environment in which the photons are emitted. The LDOS in an inhomogeneous medium is modified due to optical reflections induced by nearby interfaces and surfaces. Therefore, the decay rates measured in TRPL experiments should be compared to a modified LDOS which depends on the exact layer thicknesses and the proximity of the GaAs-vacuum interface [48,49]. Here, we have simulated the LDOS for a QD in a sample structure comprising of a GaAs substrate, a 100 nm AlGaAs charge-confinement layer, a 100 nm GaAs matrix on which the QDs are grown, and a GaAs capping layer of varying thickness. The simulations were done using the finite difference time domain (FDTD) method for a point dipole in three dimensions. The total decay rate $\Gamma(Z,\omega)$ is then the sum of the non-radiative component $\Gamma_{\mathbf{nrad}}(\omega)$ and the radiative component $\Gamma_{\mathbf{rad}}(Z,\omega)$. The radiative decay rate is, in turn, proportional to the projected LDOS $\rho(Z,\omega)$, which depends explicitly on the thickness of the cap layer Z and the optical frequency ω. We consider only the horizontal dipole orientation, which is the dominant polarization of the InAs QDs [50]. The measured total decay rate for QDs in the investigated inhomogeneous medium can thus be expressed as,

$$\Gamma(Z,\omega) = \Gamma_{\mathbf{nrad}}(\omega) + \Gamma_{\mathbf{rad}}^{\mathbf{hom}}(\omega)\frac{\rho(Z,\omega)}{\rho_{\mathbf{hom}}(\omega)} \quad (3)$$

where $\Gamma_{\mathbf{rad}}^{\mathbf{hom}}(\omega)$ is defined as the radiative decay rate for QDs in a homogenous medium and $\rho_{\mathbf{hom}}(\omega)$ is the LDOS in a homogenous medium. The decay rates were measured from QD ensembles at an emission wavelength of 950 nm (see figure S1 in supplementary information) and the data are plotted in figure 6. The decay rates obtained from as-grown QDs display good conformity with the simulation of the projected LDOS curve, even for the thinnest GaAs cap of 20 nm. The passivated QDs shown in figure 6 (b)-(d) exhibit increased decay rates for the 20 nm cap thickness, while for cap thicknesses of 30 nm or more, the data does not show statistically significant difference to the decay rates of as-grown QDs. It is clear that the differences in the decay rates between

AlN_x-passivated and as-grown QDs are small in comparison with the differences in their steady-state emission intensities (see figure 5(b)). We can therefore conclude that the improvement of the exciton emission intensity after AlN_x passivation is predominantly due to the reduction of non-radiative recombination at the GaAs-vacuum interface rather than due to a reduction of the non-radiative decay rate in the QD itself.

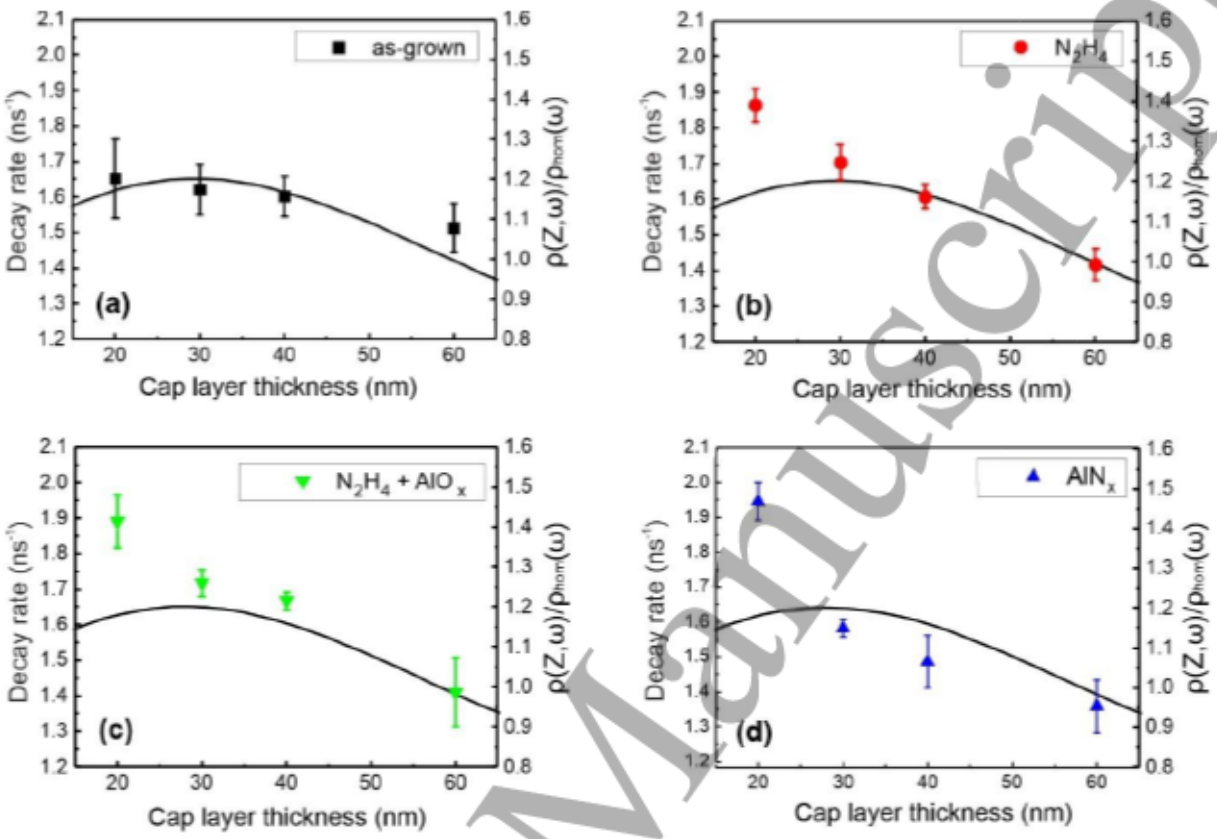

Figure 6. Decay rates plotted as a function of cap layer thickness for (a) as-grown QDs, (b) N_2H_4-passivated QDs, (c) N_2H_4 + AlO_x -passivated QDs and (d) AlN_x-passivated QDs. The decay rates are shown as the average of five measurements taken from QD ensembles at different locations on the sample and presented together with the standard deviation. The solid line in all four plots represents the FDTD-simulated LDOS for a dipole orientation parallel to the GaAs/air interface.

4. Discussions

It is important to note that all three passivation mechanisms are successful in reducing the oxidation of Ga and As atoms at the GaAs surface and, consequently, in enhancing the room-temperature PL intensity. The N_2H_4-passivated GaAs surface shows an enhancement of $634\times I_0$ initially but the passivating effect is not stable with time. This is evident from the decrease in the PL enhancement to $162\times I_0$ after one week and further to $29\times I_0$ after three months. The instability of this wet-chemistry process is most likely linked to the fact that the thickness of the passivation layer is just 1 ML in the best-case scenario. In comparison, the ALD-based methods make use of 2 nm of the passivating layer on the GaAs surface. This bring us to an initial conclusion that, in the N_2H_4 + AlO_x technique, the ALD-AlO_x overlayer stabilizes the N-passivating effect related to N_2H_4 chemical treatment. However, it is not straightforward to describe the stabilizing process of the ALD-AlO_x layer because the N_2H_4 pretreatment removes all Ga oxide, but not all As oxide (as seen from XPS results). It is the ALD-AlO_x process that then removes the rest of the As oxide and we consequently get an oxide-free interface. The N_2H_4 + AlO_x -passivated GaAs surface shows nearly the same PL enhancement after one week, suggesting an improved stability of the passivation layer. XPS measurements made one week after passivation also support this argument by showing no Ga or As oxides on the surface. Therefore, the N_2H_4 + AlO_x passivation process is more effective

because it completely removes the native oxides and prevents/diminishes further oxidation of the surface atoms for a relatively long period. Moreover, the preserving effect of ALD process is also evidenced for the ALD-AlN_x passivation method, which not only enhances PL emission by over three orders of magnitude but also maintains its passivating effect for over a year, as shown in Fig. 3(d) and in figure S2 of the supplementary information.

However, an improvement of GaAs epilayer PL intensity at room temperature does not necessarily guarantee good emission properties for QDs located close to the passivated surface. This is evident for N_2H_4 + AlO_x passivation, which has a positive effect in terms of room-temperature GaAs PL intensity but a strong detrimental effect on the exciton linewidths of individual QDs. This suggests that either the spectral diffusion caused by charge fluctuation at the surface is greatly increased or that the passivation process causes diffusion of impurities into the GaAs cap layer where they act as charge traps. Based on our results, the latter scenario is more probable because the spectral lines of individual QDs are strongly diffused even with a 60 nm GaAs cap. We also observe a direct increase in non-radiative recombination for the QDs with intermediate cap thicknesses of 30 nm and 40 nm. A typical impurity associated with the ALD growth of AlO_x is hydrogen [51], which can be present at the passivation interface and can diffuse into the GaAs cap layer. It has been shown that a well-optimized treatment of hydrogen plasma on InAs QDs improves their PL emission intensity and recombination lifetimes [52,53]. However, the results from [52] also suggest that an overdose of hydrogen can actually be detrimental to the QDs' emission properties and to the structural quality of GaAs surface. Moreover, it has also been experimentally shown that hydrogen modifies the energy structure of GaAs by creating deep, metastable states in the bandgap[54] and these deep traps could potentially influence the emission properties of nearby QDs. In such a scenario, the effect of hydrogen could possibly be remedied by well-optimized thermal annealing [55,56], which was not investigated in this study.

Ultimately, the non-radiative losses at the GaAs surface depend on the surface recombination velocity. We know from PL measurements of GaAs that the surface recombination velocity can be significantly reduced by surface passivation layers. Consequently, passivation greatly improves also the radiative efficiency of the QD-containing structures by allowing a larger number of charge carriers generated in the GaAs matrix to be captured by the QDs, where they can recombine radiatively instead of being lost to non-radiative recombination processes at the GaAs surface. This is important in terms of the overall radiative efficiency of a small-volume quantum device based on InAs/GaAs QDs, for example, a single-photon LED. On the other hand, the emission linewidths and the decay rates are directly affected by the material and surface properties and the resulting nature of the electronic structure in the immediate vicinity of the QDs. QDs respond differently to the same passivation processes (that were used for passivating bulk GaAs surface) with respect to the observed QCSE due to the charge fluctuations caused by impurities near QDs. That is, the emission properties of QDs are dependent on the interaction of excited charge carriers with the impurities present nearby as well as with the surface states near the GaAs surface. It might be intuitive to assume based on the room-temperature PL results that suppressing surface states at the GaAs surface would translate to improving the optical properties of nearby QDs. But our data from low-temperature PL experiments suggests that it is not necessarily the case, especially for QDs that are situated 30 nm or more away from the surface. Therefore, in general, different surface or impurity states can be responsible for the two processes, namely, non-radiative surface recombination and QCSE.

Most notably, the AlN_x passivation is effective in all experiments carried out in this work: it reduces oxidation of Ga and As at the GaAs surface, it improves the room-temperature PL intensity of surface-sensitive GaAs by over three orders of magnitude, owing to a reduction in surface recombination velocity by the same order of magnitude, and at the same time the enhancement in PL intensity is a permanent effect. Moreover, an essential effect for quantum technology applications is that the ALD-AlN_x process provides a passivation of the charge fluctuations. This results in the QD exciton linewidth and intensity to be nearly independent of the thickness of GaAs cap layer, if the cap thickness is 30 nm or more. Overall, this is an extremely encouraging result considering passivation of small-volume InAs/GaAs QD devices, such as QD-nanocavity systems and compact single-photon LEDs. We also observe a slight reduction of the non-radiative recombination (based on QD decay statistics) in the QDs with cap thicknesses of 30 nm or more. Therefore, the ALD-AlN_x process is a robust surface passivation technique for nanoscale quantum devices based on InAs/GaAs QDs.

5. Conclusions

We have investigated three different surface passivation methods for improving the properties of GaAs (100) surfaces and InAs QDs positioned close to such surfaces. The first method was N_2H_4-based chemical N-passivation, the second method included the ALD growth of a 2 nm AlO_x overlayer on the N_2H_4-treated surface and the third passivation method involved ALD-AlN_x passivation procedure which included a TMA and N_2 plasma pretreatment of the GaAs surface. All three methods reduce oxidation of Ga and As atoms at the surface and provide a significant enhancement of the surface-sensitive GaAs epilayer PL intensity, which indicates a strong reduction in surface recombination. The efficacy of the N_2H_4 passivation is temporary, but the N_2H_4 + AlO_x and the AlN_x passivation processes provide stable improvements in PL intensity. However, the N_2H_4 + AlO_x passivation causes a strong spectral diffusion of the QD PL emission lines. This leads us to conclude that room-temperature PL intensity is not necessarily a good indicator of the efficacy of the passivation for close-to-surface QDs. On the other hand, the ALD-AlN_x passivation is a successful passivation technique in all aspects of this study: it improves the GaAs PL intensity, reduces the surface-induced spectral diffusion in close-to-surface QDs, enhances the PL emission intensity of the QDs and reduces non-radiative recombination. Moreover, since ALD is a conformal deposition method, the AlN_x passivation can be effectively carried out on more complex geometries like micropillars and suspended-membrane photonic crystal cavities. These properties make ALD-based AlN_x passivation the ideal candidate for improving the performance of nanoscale photonic devices and cavity-QD systems based on InAs/GaAs QDs.

ORCID iDs

Abhiroop Chellu https://orcid.org/0000-0001-5965-4234

Eero Koivusalo https://orcid.org/0000-0001-5029-4658

Heli Seppänen https://orcid.org/0000-0002-5402-0758

Mircea Guina https://orcid.org/0000-0002-9317-8187

Marianna Raappana https://orcid.org/0000-0003-1034-5523

Teemu Hakkarainen https://orcid.org/0000-0001-6758-2496

Antti Tukiainen https://orcid.org/0000-0003-2227-833X

Ville Polojärvi https://orcid.org/0000-0001-9490-0672

Kimmo Lahtonen https://orcid.org/0000-0002-8138-7918

Jesse Saari https://orcid.org/0000-0001-6741-0838

Mika Valden https://orcid.org/0000-0002-9693-9818

Harri Lipsanen https://orcid.org/0000-0003-2487-4645

Sanna Ranta https://orcid.org/0000-0001-5768-8270

Acknowledgements

The authors acknowledge financial support from the Academy of Finland projects NanoLight (# 310985) and QuantSi (# 323989), and the Academy of Finland Flagship program PREIN (# 320168). H. Seppänen acknowledges the support from Walter Ahlström foundation. J. Saari acknowledges the support from the Vilho, Yrjö and Kalle Väisälä Foundation of the Finnish Academy of Science and Letters.

References

[1] Zhang Z Y, Oehler A E H, Resan B, Kurmulis S, Zhou K J, Wang Q, Mangold M, Süedmeyer T, Keller U, Weingarten K J and Hogg R A 2012 1.55 μm InAs/GaAs quantum dots and high repetition rate quantum dot SESAM mode-locked laser *Sci. Rep.* **2**

[2] Wu J, Makableh Y F M, Vasan R, Manasreh M O, Liang B, Reyner C J and Huffaker D L 2012 Strong interband transitions in InAs quantum dots solar cell *Appl. Phys. Lett.* **100**

[3] Kim H, Ahn S-Y, Kim S, Ryu G, Kyhm J H, Lee K W, Park J H and Choi W J 2017 InAs/GaAs quantum dot infrared photodetector on a Si substrate by means of metal wafer bonding and epitaxial lift-off *Opt. Express* **25** 17562–70

[4] Ding X, He Y, Duan Z C, Gregersen N, Chen M C, Unsleber S, Maier S, Schneider C, Kamp M, Höfling S, Lu C Y and Pan J W 2016 On-demand single photons with high extraction efficiency and near-unity indistinguishability from a resonantly driven quantum dot in a micropillar *Phys. Rev. Lett.* **116** 1–6

[5] Santori C, Fattal D, Vučković J, Solomon G S and Yamamoto Y 2002 Indistinguishable photons from a single-photon device *Nature* **419** 594–7

[6] Chen Y, Zhang J, Zopf M, Jung K, Zhang Y, Keil R, Ding F and Schmidt O G 2016 Wavelength-tunable entangled photons from silicon-integrated III-V quantum dots *Nat. Commun.* **7**

[7] Yoshie T, Scherer A, Hendrickson J, Khitrova G, Gibbs H M, Rupper G, Ell C, Shchekin O B and Deppe D G 2004 Vacuum Rabi splitting with a single quantum dot in a photonic crystal nanocavity *Nature* **432** 200–3

[8] Vahala K J 2003 Optical microcavities *Nature* **424** 839–46

[9] Faraon A, Fushman I, Englund D, Stoltz N, Petroff P and Vučković J 2008 Coherent generation of non-classical light on a chip via photon-induced tunnelling and blockade *Nat. Phys.* **4** 859–63

[10] Liu J, Konthasinghe K, Davanço M, Lawall J, Anant V, Verma V, Mirin R, Nam S W, Song J D, Ma B, Chen Z S, Ni H Q, Niu Z C and Srinivasan K 2018 Single self-assembled InAs/GaAs quantum dots in photonic nanostructures: the role of nanofabrication *Phys. Rev. Appl.* **9**

[11] Wang C F, Badolato A, Wilson-Rae I, Petroff P M, Hu E, Urayama J and Imamoğlu A 2004 Optical properties of single InAs quantum dots in close proximity to surfaces *Appl. Phys. Lett.* **85**

[12] Baca A and Ashby C 2005 *Fabrication of GaAs Devices* (The Institution of Engineering and Technology, Michael Faraday House, Six Hills Way, Stevenage SG1 2AY, UK: IET)

[13] Robinson H and Goldberg B 2000 Light-induced spectral diffusion in single self-assembled quantum dots *Phys. Rev. B - Condens. Matter Mater. Phys.* **61** R5086–9

[14] Blome P, Wenderoth M, Hübner M, Ulbrich R, Porsche J and Scholz F 2000 Temperature-dependent linewidth of single InP/GaInP quantum dots: Interaction with surrounding charge configurations *Phys. Rev. B - Condens. Matter Mater. Phys.* **61** 8382–7

[15] Houel J, Kuhlmann A V., Greuter L, Xue F, Poggio M, Warburton R J, Gerardot B D, Dalgarno P A, Badolato A, Petroff P M, Ludwig A, Reuter D and Wieck A D 2012 Probing single-charge fluctuations at a GaAs/AlAs interface using laser spectroscopy on a nearby InGaAs quantum dot *Phys. Rev. Lett.* **108**

[16] Wang X Y, Ma W Q, Zhang J Y, Salamo G J, Xiao M and Shih C K 2005 Photoluminescence intermittency of InGaAs/GaAs quantum dots confined in a planar microcavity *Nano Lett.* **5** 1873–7

[17] Nirmal M, Dabbousi B O, Bawendi M G, Macklin J J, Trautman J K, Harris T D and Brus L E 1996 Fluorescence intermittency in single cadmium selenide nanocrystals *Nature* **383** 802–4

[18] Kuno M, Fromm D P, Hamann H F, Gallagher A and Nesbitt D J 2000 Nonexponential "blinking" kinetics of single CdSe quantum dots: A universal power law behavior *J. Chem. Phys.* **112** 3117–20

[19] Frantsuzov P, Kuno M, Jankó B and Marcus R A 2008 Universal emission intermittency in quantum dots, nanorods and nanowires *Nat. Phys.* **4** 519–22

[20] Stefani F D, Hoogenboom J P and Barkai E 2009 Beyond quantum jumps: Blinking nanoscale light emitters *Phys. Today* **62** 34–9

[21] Davanço M, Hellberg C S, Ates S, Badolato A and Srinivasan K 2014 Multiple time scale blinking in InAs quantum dot single-photon sources *Phys. Rev. B - Condens. Matter Mater. Phys.* **89**

[22] Neuhauser R G, Shimizu K T, Woo W K, Empedocles S A and Bawendi M G 2000 Correlation between fluorescence intermittency and spectral diffusion in single semiconductor quantum dots *Phys. Rev. Lett.* **85** 3301–4

[23] Skromme B J, Sandroff C J, Yablonovitch E and Gmitter T 1987 Effects of passivating ionic films on the photoluminescence properties of GaAs *Appl. Phys. Lett.* **51** 2022–4

[24] Sandroff C J, Nottenburg R N, Bischoff J C and Bhat R 1987 Dramatic enhancement in the gain of a GaAs/AlGaAs heterostructure bipolar

transistor by surface chemical passivation *Appl. Phys. Lett.* **51** 33–5

[25] Besser R S and Helms C R 1989 Comparison of surface properties of sodium sulfide and ammonium sulfide passivation of GaAs *J. Appl. Phys.* **65** 4306–10

[26] Viktorovitch P, Gendry M, Krawczyk S K, Krafft F, Abraham P, Bekkaoui A and Monteil Y 1991 Improved electronic properties of GaAs surfaces stabilized with phosphorus *Appl. Phys. Lett.* **58** 2387–9

[27] Berkovits V L, Paget D, Karpenko A N, Ulin V P and Tereshchenko O E 2007 Soft nitridation of GaAs(100) by hydrazine sulfide solutions: Effect on surface recombination and surface barrier *Appl. Phys. Lett.* **90** 022104

[28] Berkovits V L, Ulin V P, Losurdo M, Capezzuto P, Bruno G, Perna G and Capozzi V 2002 Wet chemical nitridation of GaAs (100) by hydrazine solution for surface passivation *Appl. Phys. Lett.* **80** 3739–41

[29] Bosund M, Mattila P, Aierken A, Hakkarainen T, Koskenvaara H, Sopanen M, Airaksinen V M and Lipsanen H 2010 GaAs surface passivation by plasma-enhanced atomic-layer-deposited aluminum nitride *Appl. Surf. Sci.* **256** 7434–7

[30] Bosund M, Sajavaara T, Laitinen M, Huhtio T, Putkonen M, Airaksinen V M and Lipsanen H 2011 Properties of AlN grown by plasma enhanced atomic layer deposition *Appl. Surf. Sci.* **257** 7827–30

[31] Bosund M, Aierken A, Tiilikainen J, Hakkarainen T and Lipsanen H 2008 Passivation of GaAs surface by atomic-layer-deposited titanium nitride *Appl. Surf. Sci.* **254** 5385–9

[32] Sah R E, Driad R, Bernhardt F, Kirste L, Leancu C-C, Czap H, Benkhelifa F, Mikulla M and Ambacher O 2013 Mechanical and electrical properties of plasma and thermal atomic layer deposited Al_2O_3 films on GaAs and Si *J. Vac. Sci. Technol. A Vacuum, Surfaces, Film.* **31** 041502

[33] Xuan Y, Lin H C and Ye P D 2007 Simplified surface preparation for GaAs passivation using atomic layer-deposited high-K dielectrics *IEEE Trans. Electron Devices* **54** 1811–7

[34] Alekseev P A, Dunaevskiy M S, Ulin V P, Lvova T V., Filatov D O, Nezhdanov A V., Mashin A I and Berkovits V L 2015 Nitride Surface Passivation of GaAs Nanowires: Impact on Surface State Density *Nano Lett.* **15** 63–8

[35] Gao J, He G, Liang S, Wang D and Yang B 2018 Comparative study on in situ surface cleaning effect of intrinsic oxide-covering GaAs surface using TMA precursor and Al_2O_3 buffer layer for HfGdO gate dielectrics *J. Mater. Chem. C* **6** 2546–55

[36] DuMont J W, Marquardt A E, Cano A M and George S M 2017 Thermal Atomic Layer Etching of SiO_2 by a "Conversion-Etch" Mechanism Using Sequential Reactions of Trimethylaluminum and Hydrogen Fluoride *ACS Appl. Mater. Interfaces* **9** 10296–307

[37] Freeouf J L and Woodall J M 1981 Schottky barriers: An effective work function model *Appl. Phys. Lett.* **39** 727–9

[38] Spicer W E, Kendelewicz T, Newman N, Cao R, McCants C, Miyano K, Lindau I, Liliental-Weber Z and Weber E R 1988 The advanced unified defect model and its applications *Appl. Surf. Sci.* **33–34** 1009–29

[39] Spicer W E, Lindau I, Skeath P and Su C Y 1980 UNIFIED DEFECT MODEL AND BEYOND. *Journal of vacuum science & technology* vol 17 (American Vacuum SocietyAVS) pp 1019–27

[40] Hinkle C L, Sonnet A M, Vogel E M, McDonnell S, Hughes G J, Milojevic M, Lee B, Aguirre-Tostado F S, Choi K J, Kim H C, Kim J and Wallace R M 2008 GaAs interfacial self-cleaning by atomic layer deposition *Appl. Phys. Lett.* **92** 071901

[41] Chang Y C, Chang W H, Merckling C, Kwo J and Hong M 2013 Inversion-channel GaAs(100) metal-oxide-semiconductor field-effect-transistors using molecular beam deposited Al_2O_3 as a gate dielectric on different reconstructed surfaces *Appl. Phys. Lett.* **102** 093506

[42] Stesmans A, Nguyen S and Afanas'Ev V V. 2013 $AsGa^+$ antisites identified by electron spin resonance as a main interface defect system in thermal GaAs/native oxide structures *Appl. Phys. Lett.* **103** 162111

[43] Mettler K 1977 Photoluminescence as a tool for the study of the electronic surface properties of gallium arsenide *Appl. Phys.* **12** 75–82

[44] Liu D G, Chang K H, Lee C P, Hsu T M and Tien Y C 1992 Photoreflection study on the surface electric field of delta-doped GaAs grown by molecular beam epitaxy *J. Appl. Phys.* **72** 1468–72

[45] Misiewicz J, Sitarek P, Sęk G and Kudrawiec R 2003 Semiconductor heterostructures and device structures investigated by photoreflectance spectroscopy *Mater. Sci.* **21** 263–320

[46] Komkov O S, Pikhtin A N and Zhilyaev Y V. 2012 Photoreflectance characterization of gallium arsenide *Russ. Microelectron.* **41** 508–10

[47] Aspnes D E 1983 Recombination at semiconductor surfaces and interfaces *Surf. Sci.* **132** 406–21

[48] Stobbe S, Johansen J, Kristensen P T, Hvam J M and Lodahl P 2009 Frequency dependence of

the radiative decay rate of excitons in self-assembled quantum dots: Experiment and theory *Phys. Rev. B - Condens. Matter Mater. Phys.* **80** 1–14

[49] Johansen J, Stobbe S, Nikolaev I S, Lund-Hansen T, Kristensen P T, Hvam J M, Vos W L and Lodahl P 2008 Size dependence of the wavefunction of self-assembled InAs quantum dots from time-resolved optical measurements *Phys. Rev. B - Condens. Matter Mater. Phys.* **77** 1–4

[50] Hakkarainen T V., Luna E, Tommila J, Schramm A and Guina M 2013 Impact of the non-planar morphology of pre-patterned substrates on the structural and electronic properties of embedded site-controlled InAs quantum dots *J. Appl. Phys.* **114**

[51] Guerra-Nuñez C, Döbeli M, Michler J and Utke I 2017 Reaction and Growth Mechanisms in Al_2O_3 deposited via Atomic Layer Deposition: Elucidating the Hydrogen Source *Chem. Mater.* **29** 8690–703

[52] Jacob A P, Zhao Q X, Willander M, Ferdos F, Sadeghi M and Wang S M 2002 Hydrogen passivation of self assembled InAs quantum dots *J. Appl. Phys.* **92** 6794–8

[53] Gurioli M, Zamfirescu M, Vinattieri A, Sanguinetti S, Grilli E, Guzzi M, Mazzucato S, Polimeni A, Capizzi M, Seravalli L, Frigeri P and Franchi S 2006 Characterization of hydrogen passivated defects in strain-engineered semiconductor quantum dot structures *J. Appl. Phys.* **100**

[54] Cho H Y, Kim E K, Min S K and Lee C 1991 Role of the hydrogen atom on metastable defects in GaAs *Phys. Rev. B* **43** 14498–503

[55] Dingemans G, Einsele F, Beyer W, Van De Sanden M C M and Kessels W M M 2012 Influence of annealing and Al_2O_3 properties on the hydrogen-induced passivation of the Si/SiO_2 interface *J. Appl. Phys.* **111** 093713

[56] Bosund M 2018 *Development of atomic layer deposition processes for nanotechnology applications* (Aalto University)